ACS OMEGA

Article

http://pubs.acs.org/journal/acsodf

Development of a Method and Validation for the Quantitation of FruArg in Mice Plasma and Brain Tissue Using UPLC−MS/MS

Mitch C. Johnson,[†,‡] Hailong Song,[‡,§,∥] Jiankun Cui,[‡,§,∥] Valeri V. Mossine,[‡,⊥] Zezong Gu,[*,‡,§,∥] and C. Michael Greenlief[*,†,‡]

[†]Department of Chemistry, [‡]Center for Botanical Interaction Studies, and [⊥]Department of Biochemistry, University of Missouri, Columbia, Missouri 65211, United States

[§]Center for Translational Neuroscience and [∥]Department of Pathology & Anatomical Sciences, University of Missouri School of Medicine, Columbia, Missouri 65212, United States

Supporting Information

ABSTRACT: Aged garlic extract (AGE) is a popular nutritional supplement and is believed to promote health benefits by exhibiting antioxidant and anti-inflammatory activities and hypolipidemic and antiplatelet effects. We have previously identified *N*-α-(1-deoxy-D-fructos-1-yl)-L-arginine (FruArg) as a major contributor to the bioactivity of AGE in BV-2 microglial cells whereby it exerted a significant ability to attenuate lipopolysaccharide-induced neuroinflammatory responses and to regulate the Nrf2-mediated antioxidant response. Here, we report on a sensitive ultraperformance liquid chromatography−tandem mass spectrometry (UPLC−MS/MS) protocol that was validated for the quantitation of FruArg in mouse plasma and brain tissue samples. Solid-phase extraction was used to separate FruArg from proteins and phospholipids present in the biological fluids. Results indicated that FruArg was readily absorbed into the blood circulation of mice after intraperitoneal injections. FruArg was reliably detected in the subregions of the brain tissue postinjection, indicating that it penetrates the blood−brain barrier in subnanomolar concentrations that are sufficient for its biological activity.

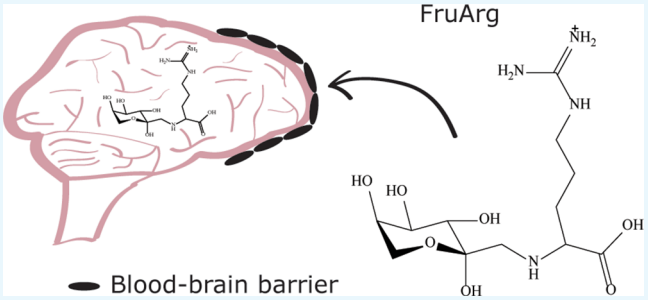

1. INTRODUCTION

The medicinal properties of garlic (*Allium sativum L.*) have long been recognized and, more recently, subjected to a large number of studies. For example, garlic was shown to protect the cardiovascular system by lowering total cholesterol in serum, by reducing supine systolic blood pressure, and by modulating platelet aggregation through upregulation of cyclic adenosine monophosphate (cAMP) in blood.[1−3] Dietary garlic may have cancer-preventive effects as well.[4,5] Thus, epidemiological studies in both Asian and Western populations established that gastric and colon cancer risks are inversely associated with garlic consumption.[6,7] One of the popular garlic nutritional supplements is aged garlic extract (AGE), an odorless product prepared by a prolonged (10−12 months) soaking of fresh garlic in 15−20% aqueous ethanol at room temperature. Health-promoting properties of AGE have been documented (for reviews see refs 8−10), and the list keeps expanding. For instance, AGE can act as a superoxide radical scavenger,[11−13] and it was shown to offer a potent antioxidant protection to cells by stimulating the activity of cellular antioxidant enzymes such as superoxide dismutase, catalase, and glutathione peroxidase and by increasing intracellular glutathione.[8,14] In humans, AGE, when delivered as a dietary supplement, reduced total serum cholesterol, low-density lipoprotein, and systolic pressure in hypercholesterolemic patients.[15]

Although the antioxidant and anti-inflammatory effects of whole AGE and its sulfur-containing constituents are reasonably well-understood, the nonsulfur nutraceuticals from AGE, such as fructose-amino acids (FAs), have not been investigated thoroughly. FAs are found in processed dairy products, dehydrated fruits, vegetables, and in medicinal preparations such as extracts from Korean red ginseng or garlic.[9,16] In addition, FAs form in vivo, largely as a result of the interaction between free glucose and N-terminal or lysine amino groups in proteins. These modified (glycated) proteins, hemoglobin A_{1c}, for example, have been used as a diagnostic marker for circulating glucose levels in metabolic diseases such as diabetes, for over 3 decades.[16−18] In spite of overwhelming evidence for constant exposure to FAs, physiological roles or significance of these compounds in humans is largely unknown. FAs are known to possess antioxidant properties, by acting either as reducing agents (e.g., electrophiles) or as chelators of redox-active metals such as copper and iron.[19−24] Reports have also demonstrated the effects of FAs as immune stimulants and the ability of FAs to prevent tumorigenesis and metastasis,

Received: September 2, 2016
Accepted: October 14, 2016
Published: October 25, 2016

DOI: 10.1021/acsomega.6b00220
ACS Omega 2016, 1, 663−668

owing to their ability to inhibit cancer cell proliferation and adhesion.[16,25,26]

One of the most abundant FAs found in AGE is *N*-α-(1-deoxy-D-fructos-1-yl)-L-arginine (FruArg), a typical Amadori rearrangement product arising from the condensation reaction between free glucose and arginine during early stages of the Maillard reaction, which is responsible for the specific color and, to a large extent, the antioxidant properties of AGE.[27,28] FruArg has been shown to exhibit antioxidant activity and hydrogen peroxide scavenging capacity that is comparable to the potent hydrogen peroxide scavenging compound ascorbic acid.[29,30] In our previous study, both AGE and FruArg exhibited a capability to modulate neuroinflammatory responses by suppressing nitric oxide (NO) production, in a concentration-dependent manner, in lipopolysaccharide-induced mouse BV-2 microglial cells without affecting the cell viability.[31] This result has thus created a pretext for further studies aiming to evaluate the potential of AGE and FruArg in targeting neuroinflammation in vivo.

A major issue in the development of drug therapy for neurological diseases is the blood−brain barrier (BBB) because more than 98% of all small molecule drugs failed to pass through the BBB to enter the brain.[32] There are certain properties a molecule must possess to be able to cross the BBB. Typically, these include a molecular weight under 500 Da and having less than 10 atoms that form hydrogen bonds.[33] As the surface area of the molecule increases, there is also a decreased likelihood that it will be able to penetrate the tight junctions formed between endothelial cells in the BBB. Several amino acids and sugars have the ability to cross the BBB.[34,35] The molecular weight of FruArg is 336, and it has 11 heteroatoms theoretically capable of participating in hydrogen bonding. However, the available crystallographic data consistently demonstrated a propensity of 3−4 heteroatoms in FAs to form strong intramolecular hydrogen bonds, whereas the furanose oxygen did not involve in any hydrogen bond formation.[36] We therefore have hypothesized that the low molecular weight and structural characteristics of FruArg may allow it to cross the BBB and enter the brain.

To enable pharmacokinetic (PK) and pharmacodynamic studies of FruArg in vivo, a reliable method for its quantification at very low concentrations is needed. A method utilizing ultraperformance liquid chromatography−electrospray ionization−tandem mass spectrometry (UPLC−ESI−MS/MS) with multiple reaction monitoring (MRM) is described. Here, we report the successful application of the validated UPLC−ESI−MS/MS method to determine the amount of FruArg in mouse plasma and in brain tissue.

2. RESULTS AND DISCUSSION

MRM transitions were identified at m/z = 337.1 → 70.1 and 337.1 → 114.1 Da and were used for the quantification and qualification of FruArg, respectively (Figure S1, upper panel). An optimized collision energy of 24 eV and an optimized cone voltage of 20 V were found. An MRM transition was identified at m/z = 155.1 → 92.1 Da and was used for the quantification of L-lysine-*d*-3,3,4,4,5,5,6,6 (L-lysine-d_8) (Figure S1, lower panel). An optimized collision energy of 13 eV and an optimized cone voltage of 24 V were found as well.

Successful separation was achieved with a UPLC gradient using perfluoropentanoic acid as an ion-pairing agent. FruArg eluted from the column at 5.9 min, and L-lysine-d_8 eluted from the column at 6.1 min (Figure 1). Excellent peak shapes and

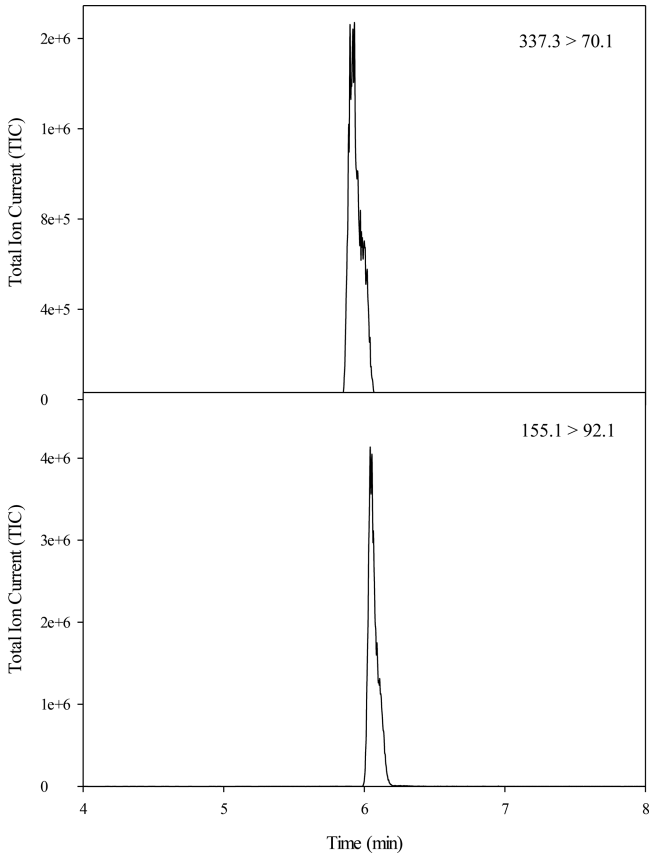

Figure 1. MRM chromatograms for FruArg and L-lysine-d_8. FruArg (top) and L-lysine-d_8 (bottom) were eluted from the column at 5.9 and 6.1 min, respectively. Their parent−daughter ion pairs were monitored as 337.3 → 70.1 and 155.1→92.1 Da, respectively. The peak areas of the MRM chromatograms were integrated and used for quantification. All FruArg concentration calculations were relative to L-lysine-d_8 I.S.

reproducible ion chromatographic peak areas and retention times were observed throughout the study. The performance of the analytical method was verified by performing a method validation. This included tests for limit of quantitation (LOQ), selectivity, linearity of the signal, range, recovery, matrix effect, and interday and intraday precision. Values for these parameters are listed in Table 1. LC-MS/MS has been used previously for the quantitation of amino acids in plasma, including studies analyzing samples from children with autism[37] and development of a method for high-throughput clinical trials.[38]

Table 1. Method Validation Parameters of Plasma and Brain Tissue[a]

	validation parameters	
	plasma	brain tissue
limit of quantitation	1 μM	0.4 μM
linearity	r^2 > 0.998	r^2 > 0.997
range	1−400 μM	0.4−200 μM
recovery	99.6%	63.3%
matrix effect	0.29%	4.3%
interday precision	CV = 6.4%	CV = 2.4%
intraday precision	CV = 4.9%	CV = 2.6%

[a]CV: coefficient of variance.

DOI: 10.1021/acsomega.6b00220
ACS Omega 2016, 1, 663−668

FruArg (40 mM) was administered intraperitoneally (2.5 μL/g body weight (BW)) to three mice. The plasma was extracted at 15, 30, 60, and 180 min and was analyzed for the FruArg concentration. The concentration of FruArg in plasma as a function of time is shown in Figure 2. At 15 min, an

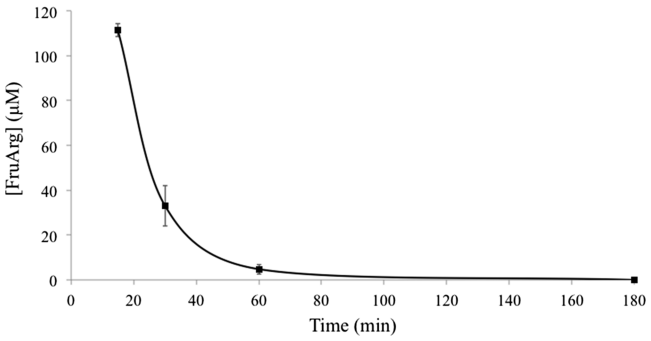

Figure 2. Plasma concentration time curve of FruArg. Concentration of FruArg in mice plasma as a function of time at 15, 30, 60, and 180 min. Individual data points are represented as the average (n = 3) FruArg concentration (μM) ± SE. The curve shown is the results from the fit of the PK data from Table 2.

average FruArg concentration of 111 ± 3 μM was observed. The FruArg concentration rapidly decreased to 33 ± 9 and 5 ± 2 μM at 30 and 60 min, respectively. At 180 min, the concentration of FruArg decreased below the LOQ. This illustrates that FruArg is rapidly absorbed into the blood stream and then distributed to other parts of the body.

PK parameters were calculated to describe the concentration−time relationship of FruArg in plasma, and the values are listed in Table 2. The initial concentration (C_0) of FruArg

Table 2. Calculated PK Parameters of FruArg in Plasma

PK parameters	
original concentration (C_0)	292 μM
elimination rate (k)	6.91×10^{-2} min^{-1}
volume distribution (VD)	2.63×10^{-3} L
half-life ($t_{1/2}$)	10.03 min
clearance (Cl)	1.8×10^{-4} L·min^{-1}
$AUC_{0\rightarrow last}$	4.86×10^{3} μM·min
$AUC_{0\rightarrow \infty}$	4.93×10^{3} μM·min

292 μM was measured by extrapolating the PK curve to 0 min. The area under the curve (AUC) measures the systemic exposure of FruArg. The ($AUC_{0\rightarrow last}$) was 4.86×10^3 μM·min, which measured the AUC from the initial concentration to the last quantifiable time point. The ($AUC_{0\rightarrow \infty}$) was 4.93×10^3 μM·min, which extrapolated the AUC from the initial concentration to infinity. The elimination rate (k) is the fraction of FruArg that is removed from the body per unit time and was 6.91×10^{-2} min^{-1}. The half-life ($t_{1/2}$) of FruArg was 10.03 min, clearance (Cl) was 1.8×10^{-4} L·min, and volume distribution (VD) was 2.63×10^{-3} L. The line shown in Figure 2 is the fit based on the PK parameters.

Brain tissue samples were collected from the cerebellum and cortex brain subregions at 15, 30, 60, and 180 min and at 15 min for the striatum and hippocampus from mice (n = 3) injected intraperitoneally (2.5 μL/g BW) with FruArg (40 mM). The concentration of FruArg as a function of time in different types of brain tissue is shown in Figure 3. FruArg was

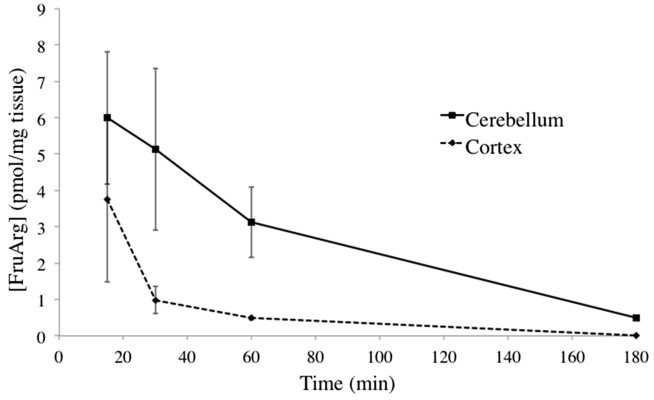

Figure 3. Brain tissue concentration time curve of FruArg in the cerebellum and cortex. Concentration of FruArg in the cerebellum (solid line) and cortex (dotted line) brain subregions as a function of time at 15, 30, 60, and 180 min. Individual data points are represented as the average (n = 3) FruArg concentration (pmol/mg tissue) ± SE.

detected in all four subregions of the brain investigated, with concentrations ranging from 4−7 pmol/mg tissue at 15 min, showing nonspecific and time-dependent character of FruArg accumulation in the brain (Table S1). Although the FruArg concentration detected in the brain is low when compared with the original injection concentration, similar results have been obtained in previous BBB studies. Gooyit et al. detected SB-3CT, a selective inhibitor of matrix metalloproteinase-2 and -9, present in similar concentrations in the brain tissue (5.0 ± 0.8 pmol/mg at 10 min), after the administration of comparable dosages to this study (25 mg/kg).[39] The dose detected in the brain may not represent the effective dose for FruArg, and further analysis of the dose range is planned.

Several strategies exist for drug delivery to the brain such as transcranial, transnasal, BBB disruption, and lipidization of small molecules. Most of these methods present major drawbacks, such as having an invasive transcranial surgery for drug delivery. The workflow of identifying molecules that can be distributed to the brain without any type of assistance could help promote an alternative form of treatment via long-term prevention. As treatments for neurological diseases advance, it is critical to consider the BBB's effect of drug delivery. FruArg has exhibited excellent anti-inflammatory responses and inhibited NO production in an in vitro model.[31] Here, we have demonstrated that FruArg is rapidly absorbed in blood, crossed the BBB, and reached all four subregions of the brain. This is somewhat unexpected because a very limited number of highly hydrophilic molecules have such an ability. Because passive penetration of the BBB by FruArg is highly unlikely, this molecule may use one of the active carbohydrate transporters, such as GLUT5. Regardless of the mechanism, our data suggest further testing of FruArg in therapeutic models aiming at prevention or treatment of neurological diseases.

3. EXPERIMENTAL SECTION

N-α-(1-Deoxy-D-fructos-1-yl)-L-arginine (FruArg) was synthesized via a reflux reaction between L-arginine and D-glucose.[40] Identification and purity of FruArg were confirmed using ^1H and ^{13}C NMR and using ESI mass spectrometry (Figure S2). A batch of purified FruArg, in the form of hydroacetate salt, was sterile-filtered and kept frozen at the stock concentration of 200 mM in double-distilled water. The stock solution at 4 °C was stable for at least 6 months. Waters IntelliStart software was

DOI: 10.1021/acsomega.6b00220
ACS Omega 2016, 1, 663−668

used to identify transitions used for MRM scans. A 10 μM FruArg standard solution was directly infused in the mass spectrometer at 20 μL/min. IntelliStart also finds the optimal collision energy and cone voltage that produces the highest number of ions. Two fragment ions of FruArg were identified; the more abundant ion was used for quantification, and the less abundant ion was used as a qualifier. L-Lysine-d_8 was used as an internal standard (I.S.) throughout the experiment. Identification of L-lysine-d_8 was verified using ESI mass spectrometry (Figure S2). A stock solution of 2000 ng/mL was prepared, and 25 μL of the stock was spiked with 25 μL of plasma or 50 μL of brain tissue initially before any sample preparation. IntelliStart was used to identify transitions for MRM scans of L-lysine-d_8 in the same manner as listed above. All quantitative measurements of FruArg were normalized to the peak areas of L-lysine-d_8 during the same LC-MS/MS run.

A Waters Acquity UPLC system equipped with a quaternary solvent manager was used in conjunction with a C18 column (Acquity BEH, 1.7 μm, 50 × 2.1 mm^2, Waters, Milford, MA, USA). A previously described 15 min UPLC method was used for FruArg separation.[41] The mobile phases used were 5 mM perfluoropentanoic acid solution in water (A) and 5 mM perfluoropentanoic acid solution in acetonitrile (B). The gradient elution was 98% A at 0 min, 98% A at 2 min, 50% A at 5 min, 50% A at 7 min, 98% A at 9 min, and 98% A at 15 min. The flow rate was 0.2 mL/min, and the injection volume was 10 μL in a full-loop mode. The column was heated to 40 °C, and the sample chamber was cooled to 10 °C.

A Waters Xevo TQ-S triple quadrupole mass spectrometer with ESI in positive-ionization mode was used. The MRM scans were conducted by selecting the parent and daughter ion m/z transitions of FruArg and L-lysine-d_8, which were optimized using IntelliStart software. The ion chromatographic peak areas of ion m/z transitions of 337.1 → 70.1 and 155.1 → 92.1 Da were monitored for FruArg and L-lysine-d_8, respectively, and the ratio of peak areas was used for quantification (Figure 1). A desolvation temperature of 350 °C and a source temperature of 150 °C were used. A capillary voltage of 2.0 kV, cone voltage of 20 V, and collision energy of 24 eV were used, and the nebulizer gas rate was 500 L N_2/h. MassLynx software (version 4.1, Waters) was used for all data acquisition.

Solid-phase extraction (SPE) was facilitated using Phree phospholipid removal solution 1 mL columns (Phenomenex). The columns were used to separate FruArg from mice plasma and brain tissue samples. The samples, 25 μL of plasma and 50 μL of brain tissue, were spiked with 25 μL of L-lysine-d_8, which was used as an I.S., and added directly on to the Phree column. Methanol (500 μL; 1% formic acid) was added to the column, and the samples were vortexed at the maximum velocity for 2 min. Vacuum pressure (5−7 mmHg) was applied, and the eluent was collected and dried under a steady stream of N_2 gas and reconstituted in 500 μL of mobile phase A.

An analytical method validation including analysis of selectivity, sensitivity, linearity, range, recovery, matrix effect, interday and intraday reproducibility was performed. Aliquots of blank plasma and brain tissue from six different mice were prepared to test the selectivity of the method. Blank plasma (25 μL) and 50 μL of blank brain tissue supernatant were prepared as mentioned below and analyzed to ensure that any potentially interfering endogenous compounds did not affect the quantification of FruArg. The signal observed for all samples was below the LOQ. The lower limit of quantitation (LLOQ) was determined by performing serial dilutions on the FruArg stock until the signal-to-noise ratio of the MRM chromatogram was approximately 10:1. Subsequent injections (n = 7) at this predicted LOQ concentration were performed, and the coefficient of variance (CV%) was determined and needed to be <20%. FruArg standards were prepared at 400, 200, 100, 50, 25, 10, 5, and 1 μM and were analyzed using the UPLC−MS/MS method discussed above to analyze the linearity and range of the analytical method. The recovery of the analytical method was analyzed for both biological matrices. Blank mice plasma (25 μL; n = 4) was spiked with 25 μL of FruArg 100 μM and 25 μL of L-lysine-d_8 (2 μg/mL) before SPE. Blank plasma (25 μL; n = 4) was spiked with equal amounts of FruArg and L-lysine-d_8 after SPE. Recovery was assessed by comparing the ratio of peak areas of FruArg/L-lysine-d_8 of the samples spiked before SPE to the ratio of peak areas of FruArg/L-lysine-d_8 spiked after SPE. The recovery of FruArg in the tissue samples was measured in the same way by spiking 50 μL of blank tissue with 25 μL of FruArg and 25 μL of L-lysine-d_8 before and after SPE. The potential matrix effects of the plasma and brain tissue were analyzed by comparing the signal of ratio of peak areas of FruArg/L-lysine-d_8 spiked after SPE to the ratio of peak areas of FruArg/L-lysine-d_8 of neat standards prepared at the same concentration but diluted from the initial FruArg stock solution in mobile phase A. Average values used for recovery and matrix effect calculations are listed in Table S2.

The precision and accuracy of this method were analyzed by performing analysis on three different batches of quality control (QC) samples over the course of 3 different days. The precision was assessed by the coefficient of variation (%) between samples (n = 3, intraday; n = 9, interday) using one-way ANOVA, and the threshold of acceptance was <15%, except at the LLOQ, where <20% is acceptable. The accuracy was assessed by calculating the mean concentration obtained for each QC level (n = 3, intraday; n = 9, interday), and the threshold of acceptance was within 15% of the calculated concentration, except at the LLOQ, where within 20% of the calculated value was acceptable. The initial FruArg stock (20 mM) was prepared in water. Serial dilutions of the initial stock were performed to obtain 200, 150, 100, 50, 25, 10, and 5 μM FruArg working stock solutions for the calibration curve. 25 μL of blank plasma was spiked with 25 μL of each concentration of working stock solution and 25 μL of L-lysine-d_8 (5 μg/mL) and was prepared by the same way as mentioned above. A calibration curve was generated using IntelliStart software, utilizing a $1/x^2$ weighting factor.

Adult male C57Bl/6J mice (The Jackson Laboratory, Bar Harbor, ME) at age 8 weeks were housed four per cage and maintained on a 12 h light/dark cycle (lights on at 7:00 AM) with unrestricted access to food and water ad libitum. Approved animal protocols were obtained in accordance with the University of Missouri and the National Institutes of Health Guidelines for the Care and Use of Laboratory Animals. Mice were injected intraperitoneally with 2.5 μL/g BW FruArg (40 mM). Terminal blood samples were collected at various time points (15 min, 30 min, 1 h, and 3 h) by cardiac puncture following CO_2 asphyxiation, using heparin as an anticoagulant. The blood was centrifuged to obtain plasma and frozen at −80 °C until use. Whole brain samples were harvested and dissected into different regions (cortex, striatum, hippocampus, and cerebellum) after transcardiac perfusion with saline and immediately flash frozen in liquid nitrogen and were stored at −80 °C until analysis. Brain samples were weighed and

DOI: 10.1021/acsomega.6b00220
ACS Omega 2016, 1, 663−668

homogenized for 5 min in 3 vol equiv of Milli-Q water using a bullet blender (Next Advance, Inc., Averill Park, NY). The homogenates were centrifuged at 12 000 rpm for 20 min at 4 °C, and the supernatants were collected and analyzed.

■ ASSOCIATED CONTENT

Supporting Information

The Supporting Information is available free of charge on the ACS Publications website at DOI: 10.1021/acsomega.6b00220.

Product ion mass spectra (MS/MS) for FruArg and L-lysine-d_8. Direct infusion mass spectra (MS) for FruArg and L-lysine-d_8. Average FruArg concentration in four brain tissue subregions at 15 min post-intraperitoneal injection. Average calculated FruArg concentrations of samples spiked before and after SPE in both plasma and brain tissue (PDF)

■ AUTHOR INFORMATION

Corresponding Authors

*E-mail: guze@health.missouri.edu. Phone: (573) 884-3880. Fax: (573) 884-4612 (Z.G.).

*E-mail: greenliefm@missouri.edu. Phone: (573) 882-3288. Fax: (573) 882-2754 (C.M.G.).

Author Contributions

Z.G. and C.M.G. conceived and designed the project. M.C.J. and H.S. performed the experiments. V.V.M. synthesized and provided the FruArg. Analyzed the data: M.C.J., H.S., J.C., Z.G., and C.M.G. Contributed reagents/materials/analysis tools: V.V.M., J.C., and C.M.G. Wrote the manuscript: M.C.J., H.S., Z.G., and C.M.G. All authors reviewed and approved the final version of the manuscript.

Notes

The authors declare no competing financial interest.

■ ACKNOWLEDGMENTS

This publication was made possible by funding of the Department of Pathology and Anatomical Sciences research fund at the University of Missouri School of Medicine (to Z.G.), as well as by Grant Number P50AT006273 from the National Center for Complementary and Integrative Health (NCCIH), the Office of Dietary Supplements (ODS), and the National Cancer Institute (NCI). Its contents are solely the responsibility of the authors and do not necessarily represent the official views of the NIEHS, NCCIH, ODS, NCI, or the National Institutes of Health.

■ REFERENCES

(1) Ried, K.; Toben, C.; Fakler, P. Effect of garlic on serum lipids: An updated meta analysis. *Nutr. Rev.* **2013**, *71*, 282−299.

(2) Stabler, S. N.; Tejani, A. M.; Huynh, F.; Fowkes, C. Garlic for the prevention of cardiovascular morbidity and mortality in hypertensive patients. *Cochrane Database Syst. Rev.* **2012**, *8*, CD007653.

(3) Rahman, K. Effects of garlic on platelet biochemistry and physiology. *Mol. Nutr. Food Res.* **2007**, *51*, 1335−1344.

(4) Amagase, H.; Schaffer, E. M.; Milner, J. A. Dietary components modify the ability of garlic to suppress 7, 12-dimethylbenz(a)-anthracene-induced mammary DNA adducts. *J. Nutr.* **1996**, *126*, 817−824.

(5) Amagase, H.; Milner, J. A. Impact of various sources of garlic and their constituents on 7,12-dimethylbenz[α]anthracene binding to mammary cell DNA. *Carcinogenesis* **1993**, *14*, 1627−1631.

(6) Woo, H. D.; Park, S.; Oh, K.; Kim, H. J.; Shin, H. R.; Moon, H. K.; Kim, J. Diet and cancer risk in the Korean population: A meta-analysis. *Asian Pac. J. Cancer Prev.* **2014**, *15*, 8509−8519.

(7) Steinmetz, K. A.; Kushi, L. H.; Bostick, R. M.; Folsom, A. R.; Potter, J. D. Vegetables, Fruit, and Colon Cancer in the Iowa Women's Health Study. *Am. J. Epidemiol* **1994**, *139*, 1−15.

(8) Borek, C. Antioxidant health effects of aged garlic extract. *J. Nutr.* **2001**, *131*, 1010S−1015S.

(9) Amagase, H. Clarifying the real bioactive constituents of garlic. *J. Nutr.* **2006**, *136*, 716S−725S.

(10) Bayan, L.; Koulivand, P. H.; Gorji, A. Garlic: A review of potential therapeutic effects. *Avicenna J. Phytomed.* **2014**, *4*, 1−14.

(11) Moriguchi, T.; Saito, H.; Nishiyama, N. Anti-ageing effect of aged garlic extract in the inbred brain atrophy mouse model. *Clin. Exp. Pharmacol. Physiol.* **1997**, *24*, 235−242.

(12) Kyo, E.; Uda, N.; Kasuga, S.; Itsakura, Y. Immunomodulatory effects of aged garlic extract. *J. Nutr.* **2001**, *131*, 1075S−1079S.

(13) Morihara, N.; Hayama, M.; Fujii, H. Aged garlic extract scavenges superoxide radicals. *Plant Foods Hum. Nutr.* **2011**, *66*, 17−21.

(14) Imai, J.; Ide, N.; Nagae, S.; Moriguchi, T.; Matsuura, H.; Itakura, Y. Antioxidant and radical scavenging effects of aged garlic extract and its constituents. *Planta Med.* **1994**, *60*, 417−420.

(15) Steiner, M.; Khan, A. H.; Holbert, D.; Lin, R. I. A double-blind crossover study in moderately hypercholesterolemic men that compared the effect of aged garlic extract and placebo administration on blood lipids. *Am. J. Clin. Nutr.* **1996**, *64*, 866−870.

(16) Mossine, V. V.; Mawhinney, T. P. 1-Amino-1-deoxy-D-fructose ("fructosamine") and its derivatives. *Adv. Carbohydr. Chem. Biochem.* **2010**, *64*, 291−402.

(17) Arif, B.; Ashraf, J. M.; Moinuddin; Ahmad, J.; Arif, Z.; Alam, K. Structural and immunological characterization of Amadori-rich human serum albumin: Role in diabetes mellitus. *Arch. Biochem. Biophys.* **2012**, *522*, 17−25.

(18) Danese, E.; Montagnana, M.; Nouvenne, A.; Lippi, G. Advantages and pitfalls of fructosamine and glycated albumin in the diagnosis and treatment of diabetes. *J. Diabetes Sci. Technol.* **2015**, *9*, 169−176.

(19) Dittrich, R.; Dragonas, C.; Kannenkeril, D.; Hoffmann, I.; Mueller, A.; Beckmann, M. W.; Pischetsrieder, M. A diet rich in Maillard reaction products protects LDL against copper induced oxidation ex vivo, a human intervention trial. *Food Res. Int.* **2009**, *42*, 1315−1322.

(20) Gyurcsik, B.; Nagy, L. Carbohydrates as ligands: Coordination equilibria and structure of the metal complexes. *Coord. Chem. Rev.* **2000**, *203*, 81−149.

(21) Ide, N.; Lau, B. H. S.; Ryu, K.; Matsuura, H.; Itakura, Y. Antioxidant effects of fructosyl arginine, a Maillard reaction product in aged garlic extract. *J. Nutr. Biochem.* **1999**, *10*, 372−376.

(22) Vhangani, L. N.; Van Wyk, J. Antioxidant activity of Maillard reaction products (MRPs) derived from fructose−lysine and ribose−lysine model systems. *Food Chem.* **2013**, *137*, 92−98.

(23) Sompong, W.; Meeprom, A.; Cheng, H.; Adisakwattana, S. A comparative study of ferulic acid on different monosaccharide-mediated protein glycation and oxidative damage in bovine serum albumin. *Molecules* **2013**, *18*, 13886−13903.

(24) Wijewickreme, A. N.; Krejpcio, Z.; Kitts, D. D. Hydroxyl scavenging activity of glucose, fructose, and ribose-lysine model Maillard products. *J. Food Sci.* **1999**, *64*, 457−461.

(25) Mossine, V. V.; Glinsky, V. V.; Mawhinney, T. P. Antitumor effects of the early Maillard reaction products. In *The Maillard Reaction: Interface between Aging, Nutrition and Metabolism*; Thomas, M. C., Forbes, J., Eds.; Royal Society of Chemistry, 2010; pp 170−179.

(26) Mossine, V. V.; Chopra, P.; Mawhinney, T. P. Interaction of tomato lycopene and ketosamine against rat prostate tumorigenesis. *Cancer Res.* **2008**, *68*, 4384−4391.

(27) Ledl, F. Chemical pathways of the Maillard reaction. In *The Maillard Reaction in Food Processing, Human Nutrition and Physiology*,

DOI: 10.1021/acsomega.6b00220
ACS Omega 2016, 1, 663−668

4th ed.; Finot, P. A., Aeschbacher, H. U., Hurrell, R. F., Liardon, R., Eds.; Birkhauser Verlag: Switzerland, 1990; pp 19−42.
(28) Martins, S. I. F. S.; Jongen, W. M. F.; van Boekel, M. A. J. S. A review of Maillard reaction in food and implications to kinetic modelling. *Trends Food Sci. Technol.* **2000**, *11*, 364−373.
(29) Ryu, K.; Ide, N.; Matsuura, H.; Itakura, Y. *N*-α-(1-deoxy-D-fructos-1-yl)-L-arginine, an antioxidant compound identified in aged garlic extract. *J. Nutr.* **2001**, *131*, 972S−976S.
(30) Ide, N.; Lau, B. H. S.; Ryu, K.; Matsuura, H.; Itakura, Y. Antioxidant effects of fructosyl arginine, a Maillard reaction product in aged garlic extract. *J. Nutr. Biochem.* **1999**, *6*, 372−376.
(31) Zhou, H.; Qu, Z.; Mossine, V. V.; Nknolise, D. L.; Li, J.; Chen, Z.; Cheng, J.; Greenlief, C. M.; Mawhinney, T. P.; Brown, P. N.; Fritsche, K. L.; Hannink, M.; Lubahn, D. B.; Sun, G. Y.; Gu, Z. Proteomic analysis of the effects of aged garlic extract and its FruArg component on lipopolysaccharide-induced neuroinflammatory response in microglial cells. *PLoS One* **2014**, *9*, No. e113531.
(32) Pardridge, W. M. The blood-brain barrier: Bottleneck in brain drug development. *NeuroRx.* **2005**, *2*, 3−14.
(33) Pardridge, W. M. Blood−brain barrier delivery. *Drug Discovery Today* **2007**, *12*, 54−61.
(34) Abbott, N. J.; Rönnbäck, L.; Hansson, E. Astrocyte−endothelial interactions at the blood−brain barrier. *Nat. Rev. Neurosci.* **2006**, *7*, 41−53.
(35) Cecchelli, R.; Berezowski, V.; Lundquist, S.; Culot, M.; Renftel, M.; Dehouck, M.-P.; Fenart, L. Modelling of the blood−brain barrier in drug discovery and development. *Nat. Rev. Drug Discovrey* **2007**, *6*, 650−661.
(36) Mossine, V. V.; Barnes, C. L.; Mawhinney, T. P. The structure of *N*-(1-deoxy-β-D-fructopyranos-1-yl)-L-proline monohydrate ("D-fructose-L-proline") and *N*-(1,6-dideoxy-α-L-fructofuranos-1-yl)-L-proline ("L-rhamnulose-L-proline"). *J. Carbohydr. Chem.* **2007**, *26*, 249−266.
(37) Tu, W.-J.; Chen, H.; He, J. Application of LC-MS/MS analysis of plasma amino acids profiles in children with autism. *J. Clin. Biochem. Nutr.* **2012**, *51*, 248−249.
(38) Harder, U.; Koletzko, B.; Peissner, W. Quantification of 22 plasma amino acids combining derivatization and ion-pair LC-MS/MS. *J. Chromatogr. B: Anal. Technol. Biomed. Life Sci.* **2011**, *879*, 495−504.
(39) Gooyit, M.; Suckow, M. A.; Schroeder, V. A.; Wolter, W. R.; Mobashery, S.; Chang, M. Selective gelitinase inhibitor neuroprotective agents cross the blood-brain barrier. *ACS Chem. Neurosci.* **2012**, *3*, 730−736.
(40) Lowy, P. H.; Borsook, H. Preparation of *N*-substituted 1-amino-1-deoxy-D-arabino-hexuloses of arginine, histidine, and lysine. *J. Am. Chem. Soc.* **1956**, *78*, 3175−3176.
(41) Troise, A. D.; Fiore, A.; Roviello, G.; Monti, S. M.; Fogliano, V. Simultaneous quantification of amino acids and Amadori products in foods through ion-pairing liquid chromatography−high-resolution mass spectrometry. *Amino Acids* **2015**, *47*, 111−124.

DOI: 10.1021/acsomega.6b00220
ACS Omega 2016, 1, 663−668